Refereed Proceedings

The 13th International Conference on Fluidization - New Paradigm in Fluidization Engineering

Engineering Conferences International *Year* 2010

NUMERICAL COMPUTATION OF HYDRODYNAMIC BEHAVIOR OF BIOMASS PARTICLES IN CIRCULATING FLUIDIZED BEDS

Afsin Gungor Dr.
Nigde University, afsingungor@hotmail.com

NUMERICAL COMPUTATION OF HYDRODYNAMIC BEHAVIOR OF BIOMASS PARTICLES IN CIRCULATING FLUIDIZED BEDS

Afsin Gungor*

Nigde University, Faculty of Engineering and Architecture, Department of Mechanical Engineering, 51100 Nigde, Turkey

ABSTRACT

A model using a particle based approach is developed to accurately predict the hydrodynamic behavior of biomass particles in CFBs. Generally, the change in the pressure gradient with height in CFB riser is small. Numerical results are in good agreement with experiments, both in form and magnitude.

INTRODUCTION

Fluidized beds have been applied widely in dealing with biomass because of their advantages of high heat transfer, uniform and controllable temperatures, favorable gas-solid contacting, and the ability to handle a wide variation in particulate properties (Lv et al., 2004). Many valuable efforts have been performed in understanding the fluidization characteristics of biomass and the mixture of biomass with fluidization medium, e.g. (Abdullah et al., 2003; Cui and Grace, 2007; Huang et al., 2006; Lv et al., 2004; Zhong et al., 2008). Good understanding and managing multiphase flows are critical to successful new energy-related processes for biomass, and to improve existing biomass processes (Cui and Grace, 2007).

In the present study a dynamic two dimensional model is developed considering the hydrodynamic behavior of biomass particles. The bottom zone in turbulent fluidization regime is modeled in detail as two-phase flow which is subdivided into a solid-free bubble phase and a solid-laden emulsion phase. In the upper zone core-annulus solids flow structure is established. Simulation model takes into account the axial and radial distribution of voidage, velocity and pressure drop for gas and solid phase, and solids volume fraction and particle size distribution for solid phase. The model results are compared with and validated against experimental data given in the literature for axial pressure profile along the bed height (Huang et al., 2006). Simulations are performed with different gas velocities at different solids mass flux values. The results are also compared with and validated against experimental data given in the literature for bed pressure drop across the riser against superficial velocity (Abdullah et al., 2003).

MODEL DESCRIPTION

The model of this paper uses particle based approach which considers the two-dimensional motion of single particles through fluids. According to the axial solid volume concentration profile, the riser is axially divided into the bottom zone and the upper zone.

* Tel.: +90 532 397 30 88; Fax: +90 388 225 01 12, E-mail: afsingungor@hotmail.com (A. Gungor)

In the present model, the bottom zone in turbulent fluidization regime is modeled as two-phase flow which is subdivided into a solid-free bubble phase and a solid-laden emulsion phase.

It is well-known that the minimum fluidization velocity is sensitive to parameters such as solid and fluid densities, the nature of solids and fluids, etc. Additionally, the minimum fluidization velocity is quite sensitive to the density difference because of the buoyancy. The particle-fluid density ratio can be related to the drag exerted from the fluid on the particles and to the void fraction. In the present work, the minimum fluidization velocity for low-effective density particulate system ($0 < \rho_{pe} < 1000\ \mathrm{kg/m^3}$) is calculated in the model as (Zhong et al., 2008);

$$u_{mf} = 1.2\times10^{-4}\left[\frac{d_{pe}^2\left(\rho_{pe}-C\right)}{\mu}\left(\frac{\rho_{pe}}{C}\right)^{1.23}\right]^{0.633} \quad (1)$$

For high-effective density particulate system ($\rho_{pe} > 1000\ \mathrm{kg/m^3}$) is calculated in the model as (Zhong et al., 2008);

$$u_{mf} = 1.45\times10^{-3}\left[\frac{d_{pe}^2\left(\rho_{pe}-C\right)}{\mu}\left(\frac{\rho_{pe}}{C}\right)^{1.23}\right]^{0.363} \quad (2)$$

where d_{pe} is the effective diameter and the following equation is used for calculating the effective particle diameter for mixtures (Zhong et al., 2008):

$$d_{pe} = d_{p1}\left[\left(\frac{\rho_1}{\rho_2}\right)\left(\frac{d_{p2}}{d_{p1}}\right)\right]^{w2/w1} = d_{p1}\left[\left(\frac{\rho_1}{\rho_2}\right)\left(\frac{d_{p2}}{d_{p1}}\right)\right]^{x2/x1} \quad (3)$$

The effective density of the mixture of biomass with fluidization medium, ρ_{pe}, is calculated using the following general equation in the model (Zhong et al., 2008):

$$\rho_{pe} = \frac{w_1\rho_1 + w_2\rho_2}{w_1 + w_2} = x_1\rho_1 + x_2\rho_2 \quad (4)$$

in which w_1 and w_2 are the weights of particles in the binary mixture, x_1 and x_2 are the mass fractions of particles in the binary mixture, with $x_1 < x_2$, and ρ_1 and ρ_2 are the densities of particles in the binary mixture. The bed porosity is calculated as $\varepsilon_{mf} = 1-\rho_b/\rho_{pe}$ in the model. In the model calculations, the effective diameter and effective density are used for biomass mixtures, and mean diameter and particle density are used for mono biomass particles.

The upper zone is located between the bottom zone and the riser exit. For the upper zone, the core-annulus flow structure is used (Smolders and Baeyens, 2001). The particles move upward in the core and downward in the annulus. Werther and Wein (1994) proposed a correlation which is further confirmed by data from large-scale CFBs. This correlation is used for the calculation of the thickness of the annulus along the riser height.

The model adopts the following simple expressions for the axial profile of the solid fraction along the upper zone. This expression is equivalent to Zenz and Weil (1958), and further confirmed by Bai and Kato (1994) for U_0 = 0.8-9 m/s, G = 4-220 kg/m^{2}s, d_p = 49-280 μm, ρ = 706-4510 kg/m^3.

$$\frac{\varepsilon - \varepsilon_{mf}}{1-\varepsilon} = \exp\left[\alpha\left(h - h_{bot}\right)\right] \tag{5}$$

where α, the decay coefficient, is a parameter to express the exponential decrease of the solid flux or solid fraction with the height and determined by the following relationship fitted by Cheng and Xiaolong (2006) with experimental data:

$$\alpha d_{pe} = 3.8\times10^{-5}\left(\frac{G_\infty}{U_0\rho_{pe}}\right)^{-0.96}\left(\frac{U_0}{\sqrt{gD}}\right)^{-0.84}\left(\frac{\rho_{pe}-C}{\rho_{pe}}\right)^{0.37} \tag{6}$$

Eq.6 reflects the relationship between the decay coefficient, gas/solid properties, flow parameters and particle size. The rate of elutriation above transfer disengaging height, G_∞, is calculated in the model as follows (Tanaka et al., 1972):

$$G_\infty = 0.046\times C\left(U_0 - U_t\right)\mathrm{Re}_p{}^{0.3}\frac{U_0 - U_t}{\sqrt{gd_{pe}}}\left(\frac{\rho_{pe}-C}{\rho_{pe}}\right)^{0.15} \tag{7}$$

The shape factor (ψ) has been widely used to quantify the shape of particles, which strongly influences their hydrodynamic behavior. It is defined as the ratio between the surface of a sphere having the same volume as the particle and the surface of particle itself. This parameter ranges from 0 to 1, being 1 for spherical particles (Reina et al., 2000). Because biomass particles commonly have more irregular shapes, in the model, average shape factor is considered as 0.45 for all biomass particle types for this study.

The gas phase is modeled as only flowing upward, backmixing of gas is neglected. The conservation of mass and momentum equations and the constitutive relations used in the model are given in Table 1.

NUMERICAL SOLUTION

The set of differential equations governing mass and momentum for the gas and solid phases are solved with a computer code developed by the author in FORTRAN language. In these equations, the dependent variables are the vertical and the horizontal components of the void fraction, the solid volume fraction, the gas pressure, the gas concentration, the vertical and the horizontal velocity components of the gas and solids. The Gauss-Seidel iteration method is used for solution procedure which contains successful relaxation method. The backward-difference method is used the discretization of the governing equations.

In terms of the dependent variables in governing equations, the pressure, the void fraction, the particle size distribution, and the superficial velocity are assigned at the

inlet boundary in the bottom zone. Other input variables are the bed geometry and the physical properties of gas and solids. No particles are allowed to leave the CFB system. A continuity condition is used for the gas phase at the top of the cyclone. The cyclone is considered as having 100% collection efficiency. In the model, recirculated particles from the cyclone are included to the solid feed particles.

RESULTS AND DISCUSSION

In order to determine the validity of the developed model in terms of axial pressure drop profile along the CFB riser, the simulation results are compared with test results using the same input variables in the tests as the simulation program input (Abdullah et al., 2003); Huang et al., 2006). It must be noted that all experiments were carried out at ambient pressure and temperature. The measurement conditions of the experimental data used for the comparison of CFB model are shown in Table 2.

Fig.1 shows the time-averaged axial pressure drop in the riser compared with experimental data for conditions of Table 2. It must be noted that the only data provided by Huang et al. (2006) considers only 8 m of height so the comparison is carried out for this data. Generally, the change in the pressure gradient with height in the bottom to the middle section (of about 8 m) is small. The absolute values of the pressure gradient decrease monotonically with increasing distance from the riser entrance and then gradually approach a constant value as clearly shown in Fig.1. However it is also possible to observe in Huang et al. (2006)'s study that since the CFB riser has an abrupt exit, particle will be reflected from the exit and accumulated in the upper and the exit regions, which will cause a positive pressure gradient along the upper and the exit regions. In the model, calculation of total pressure drop also considers the pressure drop due to distributor plate at the primary gas entrance in the bottom zone. The high pressure drop at the bottom zone is due to the effect of solid feeding in that zone as clearly seen from the Fig.1. The pressure drop then decreased along the height of the riser due to the decrease in solid concentration. The solid lines are in fair agreement with experimental data of Fig.1. The parity plots of predicted pressure drop from the proposed model against the experimental pressure drop are also included for each figure. It could be concluded from these plots that the data points obtained based on the present model are distributed evenly around and close to the parity line which illustrates the fair agreement between the proposed model predictions and the experimental data.

Figs.2-4 shows the bed pressure drop vs. superficial velocity for different bed height values which is compared with experimental data for conditions of Table 2. As the figures display, numerical results are in good agreement with experiments, both in form and magnitude. These figures show the typical fluidization curves for sawdust, rice husk and peanut shell, respectively. Abdullah et al. (2003)'s experimental study also states that sawdust and peanut shell particles have good fluidization behavior but rice husk particles have poor fluidization behavior. The parity plots of predicted pressure drop from the proposed model against the experimental pressure drop are also included for each figure. It could be concluded from these plots that the data points obtained based on the present model are distributed evenly around and close to the parity line which illustrates the fair agreement between the proposed model predictions and the experimental data.

CONCLUSIONS

In this study, a model using particle based approach is developed to accurately predict hydrodynamic behavior of biomass particles in CFBs. The model results are compared with and validated against atmospheric cold CFB experimental literature data. The pressure drop has an increasing trend along the acceleration region as the solid circulation flux increases and the superficial velocity decreases in this region.

NOTATION

C	Gas concentration, kg/m^3
C_D	Drag coefficient
d_p	Sphere mean diameter or volume sphere equivalent diameter, m
d_{pe}	Effective particle diameter of binary mixtures, m
d_{p1}, d_{p2}	Effective particle diameter of composition in binary mixtures, m
D	Riser diameter, m
G	Solids Mass flux, kg/m^2 s
$G(\varepsilon)$	Solid stress modulus, N/m^2
g	Gravity, m/s^2
h	Height above the distributor, m
h_{bot}	Bottom zone height, m
MW	Molecular weight, kg/kmol
P	Pressure, kPa
R_u	Universal gas constant, kj/kmol K
r	Radial distance from riser axis, m
Re	Reynolds number
U_0	Superficial gas velocity, m/s
U_{mf}	Minimum fluidization velocity, m/s
U_t	Transport velocity, m
u	Gas velocity, m/s
v	Particle velocity, m/s
x_b	Mass fraction of the larger particles in the binary mixture

Greek Letters

β	Gas-solid friction coefficient
ε	Void fraction
ρ_b	Bed density, kg/m^3
ρ_p	Particle density, kg/m^3
ρ_{pe}	Effective particle density, kg/m^3
μ	Viscosity, Pa s
τ	Shear stress, N/m^2

ACKNOWLEDGMENT

Financial support from the Scientific and Technical Research Council of Turkey (TUBITAK 109M167) is sincerely acknowledged.

REFERENCES

Abdullah, M. Z., Husain, Z., and Yin Pong, S. L. (2003). "Analysis of cold flow fluidization test results for various biomass fuels." **Biomass Bioenergy,** 24, 487-494.
Bai, D. R. and Kato, K. (1994). "Generalized correlations of solid holdups at dense and dilute regions of circulating fluidized beds." **Proc. 7th SCEJ Symp. CFB,** SCEJ, Tokyo, Japan, 137-144.
Chen, Y. and Xiaolong, G. (2006). "Dynamic modeling and simulation of a 410 t/h pyroflow CFB boiler." **Comp. Chem. Eng.,** 31, 21-31.
Cui, H., Grace, J. R. (2007). "Fluidization of biomass particles: A review of experimental multiphase flow aspects." **Chem. Eng. Sci.,** 62(1-2), 45-55.
Ganser, G. H. (1993). "A rational approach to drag prediction of spherical and non-spherical particles." **Powder Technol.,** 77, 143–152.
Huang, Y., Turton, R., Park, J., Famouri, P., and Boyle, E. J. (2006). "Dynamic model of the riser in circulating fluidized bed." **Powder Technol.,** 163(1-2), 23-31.
Lv, P. M., Xiong, Z. H., Chang, J., Wu, C. Z., Chen, Y., and Zhu, J. X. (2004). "An experimental study on biomass air-steam gasification in a fluidized bed." **Biores. Technol.,** 95, 95–101.
Reina, J., Velo, E., and Puigjaner, L. (2000). "Predicting the minimum fluidization velocity of polydisperse mixtures of scrap-wood particles." **Powder Technol.,** 111, 245-251.
Tanaka, I., Shinohara, H., Hirasue, H., and Tanaka, Y. (1972). "Elutriation of fines from fluidized bed." **J. Chem. Eng. Jpn.,** 5, 51-57.
Wang, W. and Li, Y. (2001). "Hydrodynamics simulation of fluidization by using a modified kinetic theory." **Ind. Eng. Chem. Res.,** 40, 5066-5073.
Wen, C. Y. and Yu, Y. H. (1966). "Mechanics of fluidization." **Chem. Eng. Progr. Symp. Ser.,** 62, 100-110.
Werther J. and Wein, J. (1994). "Expansion behavior of gas fluidized beds in the turbulent regime." **AIChE Symp. Ser.,** 301(90), 31-44.
Zenz, F. A. and Weil, N. A. (1958). "A theoretical-empirical approach to the mechanism of particle entrainment from fluidized beds." **AIChE J.,** 4, 472-479.
Zhong, W., Jin, B., Zhang, Y., Wang, X., and Xiao, R. (2008). "Fluidization of biomass particles in a gas-solid fluidized bed." **Energy Fuels**, 22(6), 4170–4176.

FIGURES

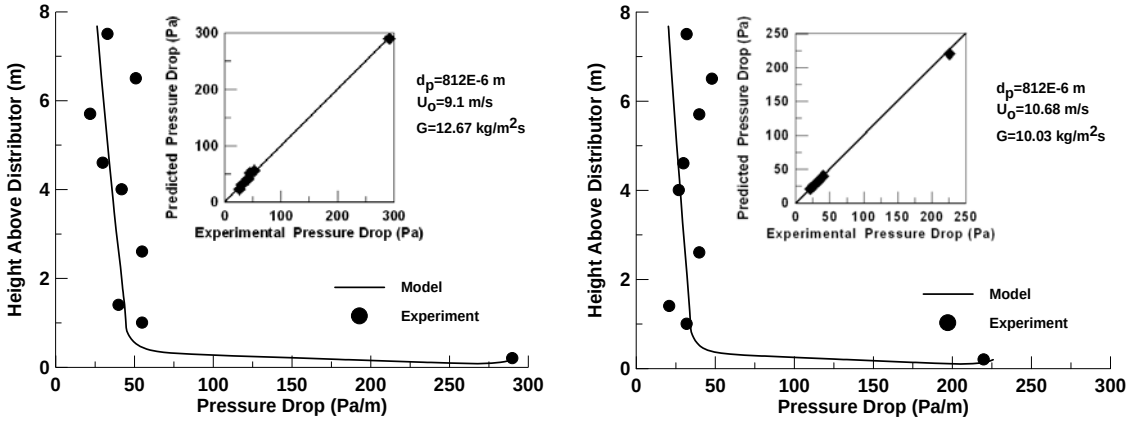

Fig.1. Comparison of model predictions with Huang et al. (2006)'s experimental data.

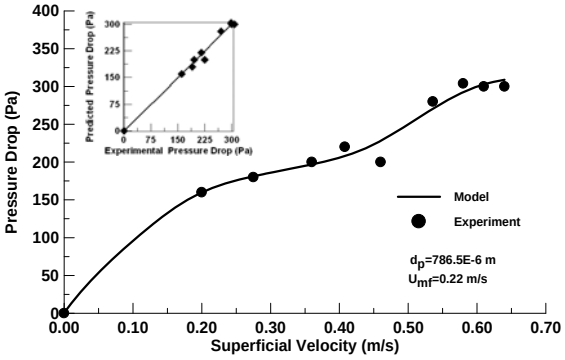

Fig.2. Comparison of model pressure drop values vs. superficial velocity for a bed height of 900 mm for sawdust with Abdullah et al. (2003)'s experimental data.

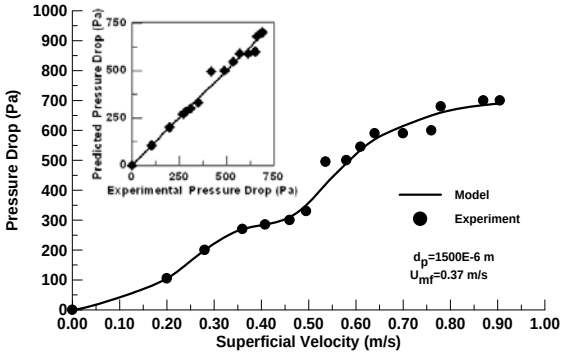

Fig.3. Comparison of model pressure drop values vs. superficial velocity for a bed height of 120 mm for rice husk with Abdullah et al. (2003)'s experimental data.

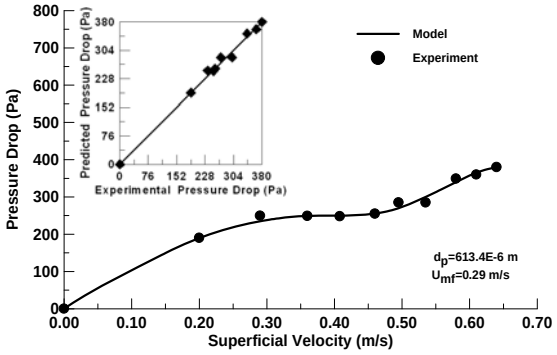

Fig.4. Comparison of model pressure drop values vs. superficial velocity for a bed height of 120 mm for peanut shell with Abdullah et al. (2003)'s experimental data.

TABLES

Table 1. The conservation of mass and momentum equations and the constitutive relations used in this study.

Gas phase	Solid phase
Continuity Equation	
$\frac{\partial(C\varepsilon)}{\partial t}+\frac{\partial(Cu\varepsilon)}{\partial r}+\frac{\partial(Cu\varepsilon)}{\partial z}=0$	$\frac{\partial(\rho_{pe}\varepsilon_p)}{\partial t}+\frac{\partial(\rho_{pe}v\varepsilon_p)}{\partial r}+\frac{\partial(\rho_{pe}v\varepsilon_p)}{\partial z}=0$
Momentum Equation	
$\frac{\partial(Cu\varepsilon)}{\partial t}+\frac{\partial(Cu\varepsilon u)}{\partial r}=-\frac{\partial(P\varepsilon)}{\partial r}-\frac{\partial(\tau_{rr}\varepsilon)}{\partial r}-\frac{\partial(\tau_{rz}\varepsilon)}{\partial z}-\beta(u-v)$ $\frac{\partial(Cu\varepsilon)}{\partial t}+\frac{\partial(Cu\varepsilon u)}{\partial z}=-\frac{\partial(P\varepsilon)}{\partial z}-\frac{\partial(\tau_{zz}\varepsilon)}{\partial z}-\frac{\partial(\tau_{zr}\varepsilon)}{\partial r}-\beta(u-v)$ $\tau_{rr}=2\mu\frac{\partial u}{\partial r}-\frac{2}{3}\mu\left(\frac{\partial u}{\partial r}+\frac{\partial u}{\partial z}\right)$ $\tau_{zz}=2\mu\frac{\partial u}{\partial z}-\frac{2}{3}\mu\left(\frac{\partial u}{\partial z}+\frac{\partial u}{\partial r}\right)$ $\tau_{rz}=\tau_{zr}=\mu\left(\frac{\partial u}{\partial z}+\frac{\partial u}{\partial r}\right)$	$\frac{\partial(\rho_{pe}v\varepsilon_p)}{\partial t}+\frac{\partial(\rho_{pe}v\varepsilon_p v)}{\partial r}=-\frac{\partial(\tau_{rr}\varepsilon_p)}{\partial r}-\frac{\partial(\tau_{rz}\varepsilon_p)}{\partial z}+\beta(u-v)-\frac{\partial(G(\varepsilon)\varepsilon_p)}{\partial r}$ $\frac{\partial(\rho_{pe}v\varepsilon_p)}{\partial t}+\frac{\partial(\rho_{pe}v\varepsilon_p v)}{\partial z}=-\frac{\partial(\tau_{zz}\varepsilon_p)}{\partial z}-\frac{\partial(\tau_{zr}\varepsilon_p)}{\partial r}+\beta(u-v)-\frac{\partial(G(\varepsilon)\varepsilon_p)}{\partial z}+\rho_{pe}g\varepsilon_p$ $\tau_{rr}=2\mu_p\frac{\partial v}{\partial r}-\frac{2}{3}\mu_p\left(\frac{\partial v}{\partial r}+\frac{\partial v}{\partial z}\right)$ $\tau_{zz}=2\mu_p\frac{\partial v}{\partial z}-\frac{2}{3}\mu_p\left(\frac{\partial v}{\partial z}+\frac{\partial v}{\partial r}\right)$ $\tau_{rz}=\tau_{zr}=\mu_p\left(\frac{\partial v}{\partial z}+\frac{\partial v}{\partial r}\right)$ **Solids stres modulus (Wang and Li, 2001);** $G(\varepsilon)=\frac{\partial\tau}{\partial(1-\varepsilon)}=10^{-8.76\cdot\varepsilon+5.43}$ **Solid-phase shear viscosity (Wang and Li, 2001);** $\mu_p=\frac{5}{96}\rho_{pe}d_{pe}\sqrt{\pi T}$
Ideal gas equation $C=\frac{MW_{air}}{R_u}\frac{P}{T}$ $MW_{air}=28.85\ kg/kmol$	
Gas-solid friction coefficient (Wen and Yu, 1996); $\beta=\frac{3}{4}C_D\frac{C\varepsilon(1-\varepsilon)}{\varepsilon^{2.65}}\frac{1}{d_{pe}}\lvert u-v\rvert$	**Drag coefficient (Ganser, 1993)** $C_D=\frac{24}{\mathrm{Re}_p K_1}\left(1+0.1125\left[\mathrm{Re}_p K_1K_2\right]^{0.657}\right)+\frac{0.431K_2}{1+3310/\mathrm{Re}_p K_1K_2}$ $\mathrm{Re}_p K_1K_2<10^5$ **For isometric particles, the shape factors are;** $K_1=\left(\frac{1}{3}+\frac{2}{3}\psi^{-0.5}\right)^{-1}$ $\log K_2=1.815(-\log\psi)^{0.574}$ $\mathrm{Re}_p=\frac{\rho_{pe}\times U_0\times D}{\mu}$

Table 2. Measurement conditions of the experimental data referred to in this study.

Author(s)	Particle Type	Bed Temp. T(°C)	Bed Diameter D(m)	Bed Height H(m)	Superficial Velocity U_0(m/s)	Particle Diameter d_p(μm)	Particle Density ρ(kg/m^3)	Bed porosity ε_{mf}
Abdullah et al. (2003)	Sawdust	25	0.06	0.90	0-1.02	786.5	570.3	0.577
	Rice husk			0.12		1500.0	630.1	0.800
	Peanut shell					613.4	566.8	0.559
Huang et al. (2006)	Cork	25	0.305	15.45	9.1-10.68	812	189.0	0.48

KEYWORDS

Biomass, Fluidization, Fluidized Bed, Hydrodynamics, Numerical Simulation, Modeling